Deltares

Comparing parametrization of Offshore Wind Farm mixing in Delft3D-FM with CFD

Comparing parametrization of Offshore Wind Farm mixing in Delft3D-FM with CFD

Auteur(s)
Luka Jaksic
Lynyrd de Wit
Leo Leummens

Comparing parametrization of Offshore Wind Farm mixing in Delft3D-FM with CFD

Opdrachtgever	Rijkswaterstaat Water, Verkeer en Leefomgeving
Contactpersoon	Edwin Verduin
Projectreferenties	SITO-PS IenW 2025 WBK09
Trefwoorden	Offshore wind; model validation; Wozep

Documentgegevens	
Versie	1.1
Datum	19-12-2025
Projectnummer	11211547-003
Document ID	11211547-003-ZKS-0001
Pagina's	33
Classificatie	
Status	Definitief

Auteur(s)		
	Luka Jaksic	
	Lynyrd de Wit	
	Leo Leummens	

Gebruik van deze tabel is voor de controle van de juiste uitvoering door Deltares van de opdracht. Ieder ander klantgebruik en externe verspreiding is niet toegestaan.

Doc. Versie	**Auteur**	**Controle**	**Akkoord**
1.0	Luka Jaksic	Erik Hendriks	Joost Icke
	Lynyrd de Wit		
	Leo Leummens		

Summary

Offshore wind turbines generate hydrodynamic wakes where the flow velocity decreases and turbulent mixing increases. This enhanced mixing may affect stratification and with it the water quality and primary production. In the Offshore Wind Ecological Programme (Wozep), we investigate these effects at North Sea basin scale with the coarse-grid Dutch Continental Shelf model in Delft3D-FM (DCSM-FM). The model does not resolve single monopile wakes but their cumulative effect on the scale of entire offshore windfarms (OWFs). This is done by imposing a friction term in the hydrodynamic model, i.e. a parametrization of the monopile influence, inside the wind farms. Because detailed spatial field data on monopile mixing are lacking, it is uncertain whether the modelled OWF mixing and its ecological effects reflect real conditions.

In anticipation of adequate field data, this study assesses how the OWF mixing parametrization in the DCSM-FM compares to that in a high-resolution Computational Fluid Dynamics (CFD) model. A CFD model can simulate the wake of individual monopiles in much more detail and accuracy than models in Delft3D-FM. The advantage of CFD over field data is that the data is free of strong natural variability and that a range of idealized conditions could be imposed. For the comparison of DCSM-FM with CFD, both models can be run with identical conditions.

Simulations are performed with a numerical flume that is one kilometre wide and one to three kilometres long, containing one to three monopiles. Each simulation is performed with CFD, using a fine grid that captures turbulent mixing of individual monopiles, and a Delft3D-FM model configured with the same grid size (1 x 1 km) and OWF parametrization as in Wozep's DCSM-FM model. The comparison of CFD results with available field measurements shows that CFD simulations reproduce realistic monopile-induced mixing, where stratification decay and wake expansion are consistent with observations. The CFD results highlight the importance of accounting for spatial variability when comparing coarse-grid DCSM-FM results with higher-resolution data from field surveys or Earth Observations, as the OWF effect in area-averaged data is strongly diminished by the inherent spatial averaging.

For the idealized test conditions, the DCSM-FM OWF mixing parametrization overestimates stratification decline by a factor of three to five compared to CFD. In agreement with literature, sensitivity tests indicate that reducing the drag coefficient from the default value of 0.7 to 0.3, more than halves the stratification decline. Although this improves agreement with CFD, 0.3 is lower than drag coefficients commonly applied in large-scale OWF studies.

Furthermore, Wozep's hydrodynamic model in Delft3D-FM predicts continued stratification decline several kilometers downstream of the last monopile, likely due to advection of turbulent kinetic energy, whereas CFD shows this effect vanishing after a few hundred meters.

Monopile orientation also subtly influences mixing in CFD, with interacting wakes reducing efficiency per monopile—an effect not captured in Wozep's current approach, where the turbulence production is proportional to the monopile surface area per cell regardless of the orientation.
Based on these findings, we recommend an end-to-end review of the OWF mixing parametrization, including the code implementation of processes such as advection of turbulent kinetic energy and the sensitivity to key model parameters. First, we advise exploring the bandwidth within which the water-quality results may be influenced. Furthermore, we recommend validating CFD-based insights with observational and model data under more realistic spatial and temporal varying conditions (e.g. wake interactions, cumulative effects for a complete wind farm).

Content

1 Introduction

1.1 *Context:* impact validation offshore wind

Within the Offshore Wind Ecology program (Wozep), Deltares applies numerical models to assess ecosystem effects of future scenarios for offshore wind. In these scenarios, offshore wind capacity is scaled up to as much as 200 GW by 2040. Validation of the modelled Offshore Wind Farm (OWF) impacts is the main priority in Wozep for the coming years. This study contributes to this validation effort, by examining the OWF mixing parametrization applied in the Wozep models.

1.2 Why offshore wind farm mixing matters

Monopiles interact with ambient currents, generating turbulent mixing and thereby influencing water column stratification, as well as the transport of fine sediments and nutrients. These shifts affect the underwater light climate and nutrient availability, which are key drivers of phytoplankton growth and thus the food availability in marine ecosystems (van Duren, et al., 2021; Zijl, et al., 2023; van Duren, et al., 2025). Therefore, accurately modelling OWF-induced mixing is essential for predicting ecological impacts linked to changes in stratification.

Previous Wozep model studies showed that large-scale offshore wind development can substantially affect primary production in the North Sea. In some regions, OWF enhanced mixing increases nutrient availability in surface waters, stimulating primary production. In others, with stronger OWF mixing or less stratification, enhanced mixing leads to higher fine sediment concentration in the upper water layers. This then leads to increased turbidity, affecting light climate and thus reduced primary production. The balance between nutrient enrichment and light limitation is steered by mixing and ultimately determines the net effect on primary production.

1.3 Evaluating OWF mixing parametrization with CFD results

The Dutch Continental Shelf Model (DCSM) is applied in Wozep to model OWF effects in the North Sea (van Duren, et al., 2025). The model has a horizontal resolution of about 1 km which is much larger than the diameter of monopiles which is order ~10 m. In Wozep's DCSM-FM model, the effect of individual monopile wakes is not modeled. Instead, the cumulative effect of these wakes is represented on the scale of entire OWFs by parametrizing their effect on the flow field. At present, it is not known if the modelled turbulent mixing caused by OWFs in DCSM-FM is representative for actual conditions.

Ideally, Wozep's DCSM-FM models would be compared directly with field data. However, in absence of field data with sufficient detail and field data is always influenced by natural variability, we use high-resolution Computational Fluid Dynamics (CFD) simulations to compare the OWF mixing parameterization in the Wozep models against. The advantage of CFD compared to field measurements is that the data is free of strong natural variability and that a wide range of idealized conditions can be imposed. For example with respect to amount of stratification, number of monopiles and depth variation. This makes CFD a valuable tool for understanding fine-scale processes and for validating or informing the parameterizations used in the coarser DCSM-FM models. Bridging the associated spatial scale difference is also essential for designing and interpreting future field measurements aimed at validating OWF-induced mixing in the Wozep model framework.

Unlike large-scale models, CFD simulations can resolve turbulent mixing by OWFs explicitly, without relying on parametrizations. The comparison can help indicate whether refinements to the Wozep model are warranted for future impact assessments of offshore wind developments.

1.4 Approach & reader's guide

To enable a fair comparison between Wozep's DCSM-FM model and the CFD model, this study uses a numerical flume setup — an idealized flow domain where conditions such as depth, initial stratification, current velocity, and turbine density can be prescribed identically in both models. Several parameters are varied, including turbine number, spacing (side-by-side vs. in-line), and model calibration coefficients, to test how well the Wozep's OWF mixing parametrization compares to the CFD results.

Chapter 2.3 presents the theoretical background of the OWF mixing parametrization used in Wozep, including its governing equations, main assumptions, and software implementation. It also provides an overview of the CFD model used as a high-resolution reference, including the key assumptions and turbulence treatment. Chapter 3 presents the numerical flume setup and simulations applied in both models. Finally, the results of this comparison are discussed in Chapter 4, followed by conclusions and recommendations in Chapter 5.

2 Theoretical background

To understand how Offshore Wind Farm (OWF) mixing is parametrized in Wozep, it is crucial to understand how turbulence is modelled in large-scale models (Section 2.1). Sections 2.2 and 2.3 then present the parametrization of OWF effects used in Wozep and the CFD modeling framework, respectively.

2.1 Resolving versus parametrizing turbulence

Underwater mixing occurs when flows interact with the seabed, other currents, or obstacles such as monopiles, generating turbulence in the form of vortices or eddies. Turbulent eddies mix vertical and horizontal gradients of salinity, temperature, nutrients, and suspended sediments—modifying water column stratification, turbidity, and nutrient distribution. Larger eddies break down into smaller ones, and eventually into fine-scale turbulence that dissipates energy as heat. This process is known as the energy cascade, schematized in Figure 2-1 (left panels), where most energy is contained in the large eddies (low wavenumbers, k) and is gradually transferred to smaller scales (higher wavenumber, k).

High-resolution CFD models with sufficiently fine grids can explicitly resolve most turbulent eddies generated by flow interaction with monopiles. The drag imposed by the monopiles slows down and separates the flow, producing large eddies that mix the surrounding water. When performing DNS (Direct Numerical Simulation) all turbulent eddies are resolved and an ultra fine grid is required to resolve even the smallest turbulent Kolmogorov scales. For field cases with high Reynolds numbers this is not feasible. Hence, most studies employ a LES (Large Eddy Simulation) approach. In LES the larger turbulent scales, which contain most of the total turbulent kinetic energy, are resolved and only the smallest scales require a subgrid[1] parametrization (bottom row, Figure 2-1). Because the increased turbulence generated by a monopile arises naturally from the resolved flow, no additional wind farm parametrization is needed.

In contrast, coarse-grid models like the one used in Wozep, cannot resolve the onset of turbulence around individual monopiles. Instead, they typically use a parameterization to slow down the mean flow combined with a RANS (Reynolds-Averaged Navier–Stokes) turbulence closure, where all turbulent energy and its mixing effect are parametrized rather than resolved (top row, Figure 2-1). The parametrization used in Wozep is discussed in the following Section 2.2.

[1] Subgrid refers to processes that occur at a finer spatial resolution than the computational model grid.

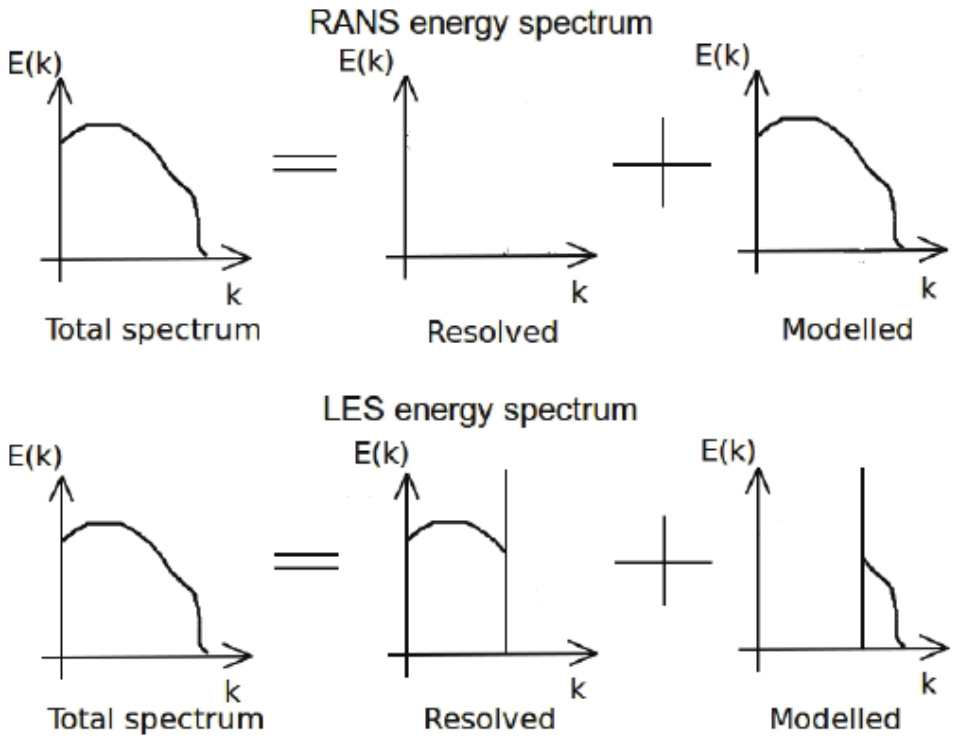

Figure 2-1 Difference in turbulence modelling approach for coarse-grid, RANS-type models (top) and fine-grid, LES-CFD type models (bottom). The resolved or modelled turbulent kinetic energy E is shown on the y-axis for different spatial scales on the x-axis. High wavenumbers k (x-axis) denote smaller spatial scales. From Füle & Hernádi (2014).

2.2 Monopile parameterization in Wozep's DCSM-FM model

The Dutch Continental Shelf Model (DCSM) that is applied in Wozep runs on the Delft3D-FM software that solves the Reynolds-Averaged Navier–Stokes (RANS) equations using the Boussinesq and hydrostatic assumptions. For turbulence closure, the $k-\epsilon$ model is used, in which k is the turbulent kinetic energy and ϵ represent the rate of dissipation of turbulent kinetic energy (Deltares, 2025).

Because the model's horizontal resolution is much larger (~1km) than the diameter of monopiles (~10m), their effects on the main flow are approximated using the action-reaction principle. The total drag force decelerating the main flow $\boldsymbol{F_d}$ (N/m^3) is assumed to be proportional to the surface area of all monopiles in one computational cell (Equation 2-1):

$$\boldsymbol{F_d}(z) = \frac{1}{2}\,\rho_0\, C_D\, \phi(z)\, n(z)\, |\boldsymbol{u}(z)|\boldsymbol{u}(z) \quad \textit{(2-1)}$$

with ρ_0 the water density (kg/m^3), C_D the cylindrical drag coefficient $(-)$, ϕ the pile width (m), n the number of piles per unit area (m^{-2}) and $\boldsymbol{u}$ the horizontal flow velocity vector (m/s). In the Wozep DCSM model C_D is set at 0.7, which gave a good comparison to experiments with a dense field of submerged rigid cylinders (Meijer, 1998; Kernkamp, 2021). The value of C_D is important calibration coefficient for the modelled influence of monopiles and depends amongst others on the monopile design, depth and marine growth (Christiansen et al., 2023).

An important assumption in Equation 2-1 is that the orientation and position of monopiles within a computational cell do not affect the total drag force. In other words, it makes no difference whether the monopiles are aligned with the flow direction or positioned side-by-side.

The drag force imposes a deceleration of the main flow, which is illustrated in Equation 2-2 for the momentum equation in x-direction (negative, green term). The energy lost due to drag is transferred into the production of turbulent kinetic energy k and its dissipation ϵ in the turbulence closure model, which affect the flow through the eddy viscosity parameter ν_v (purple term, Eq. 2-2). The magnitude of ν_V follows from k and ϵ, as described in Equation 2-3.

$$\frac{\partial u}{\partial t} + u\frac{\partial u}{\partial x} + v\frac{\partial u}{\partial y} + w\frac{\partial u}{\partial z} = fv - \frac{1}{\rho_0}\frac{\partial P}{\partial x} + F_x + \frac{\partial}{\partial z}\left(\nu_V \frac{\partial u}{\partial z}\right) + M_x - F_{d,x} \tag{2-2}$$

Turbulence closure (over $\nu_V \frac{\partial u}{\partial z}$)

Mixing (over $\frac{\partial}{\partial z}\left(\nu_V \frac{\partial u}{\partial z}\right)$) *Turbine drag* (over $F_{d,x}$)

A larger eddy viscosity ν_v represents stronger mixing of momentum (purple term in Eq. 2-2) and, through its relation to the eddy diffusivity D_v (Eq. 2-4), enhances vertical mixing of heat, salinity, and density stratification.

$$\nu_V = c_\mu \frac{k^2}{\epsilon} \qquad (2\text{-}3) \qquad D_v = \frac{\nu_V}{\sigma_c} \qquad (2\text{-}4)$$

where c_μ and σ_c are constants, with σ_c representing the Prandl-Schmidt constant.

Turbulent kinetic energy k and its dissipation ϵ follow from the differential equations of the $k-\epsilon$ closure model (Equations 2-5 and 2-6), in which the highlighted terms account for the OWF effects. The assumption in Equation 2-5 is that the generation of turbulent energy equals the kinetic energy loss caused by the presence of wind farms. This is essentially the work done by the OWF drag force $\boldsymbol{F_d}$ (blue term Eq. 2-5).

$$\frac{\partial k}{\partial t} = \frac{1}{1-A_p}\frac{\partial}{\partial z}\left\{\left(1-A_p\right)\left(\nu + \frac{\nu_t}{\sigma_k}\right)\frac{\partial k}{\partial z}\right\} + \boldsymbol{F_d}\,\boldsymbol{u} + P_k - B_k - \varepsilon \qquad (2\text{-}5)$$

$$\frac{\partial \varepsilon}{\partial t} = \frac{1}{1-A_p}\frac{\partial}{\partial z}\left\{\left(1-A_p\right)\left(\nu + \frac{\nu_t}{\sigma_k}\right)\frac{\partial \varepsilon}{\partial z}\right\} + \boldsymbol{F_d}\,\boldsymbol{u}\,\tau^{-1} + P_\varepsilon - B_\varepsilon - \varepsilon_\varepsilon \qquad (2\text{-}6)$$

Dissipation is furthermore governed by a turbulent dissipation time scale τ (red term Eq. 2-6), with $\tau = \min\left(\tau_{free}, \tau_{veg}\right)$ – as defined in Eq. 2-7 and 2-8:

$$\tau_{free} = \frac{1}{c_{2\epsilon}}\frac{k}{\epsilon} \qquad (2\text{-}7) \qquad \tau_{veg} = \frac{1}{c_{2\epsilon}\sqrt{c_\mu}}\sqrt[3]{\frac{L^2}{F_d}} \qquad (2\text{-}8) \qquad L = C_l\sqrt{\frac{1-A_p}{n}} \qquad (2\text{-}9)$$

, where $c_{2\epsilon}$ and c_μ are model weighting parameters.

For low-density applications such as offshore wind farms, the dissipation time scale is primarily governed by the unrestricted turbulence time scale τ_{free} (Eq. 2-7). Time scale τ_{veg} is included in the model to automatically account for applications where turbulence is limited by the distance between stems, such as dense vegetation fields (Eq. 2-8). Length scale L represents the smallest distance between stems, and is calculated with the stem area A_p, stem density n

and a reduction coefficient C_l (Eq. 2-9). In previous Wozep studies, C_l was set at 0.8, which is found applicable for vegetation (Uittenbogaard, 2000).

It can be concluded that the presented OWF parametrization in this section depends on different physics-based model parameters. In a sensitivity study, Christiansen et al. (2023) show that C_D has the strongest influence on turbulence production and decay of stratification (see Eq. 2-1). They show that turbulence production can increase as much as a factor 4.6 by increasing C_D from 0.35 to 1. Generic literature for flow past a single round pile, see Figure 2-2, provides a range of C_D values between ~0.1-0.3 for smooth piles and ~0.35-0.45 for rough piles for Reynolds ~10^6-10^7 which is the range for monopiles with a diameter of ~10m. For OWF applications, Carpenter et al. (2016) mention a wider range of 0.35 to 1, but even higher C_D values are applied, such as 1.1 in a high-resolution model study by Denis et al. (2025). Therefore, the Wozep value of C_D = 0.7 fits nicely in the middle of the reported range. Furthermore, it aligns well with Rennau et al. (2012), who apply $C_D = 0.65$ in a numerical model with a similar grid resolution as the one applied in Wozep (~1km).

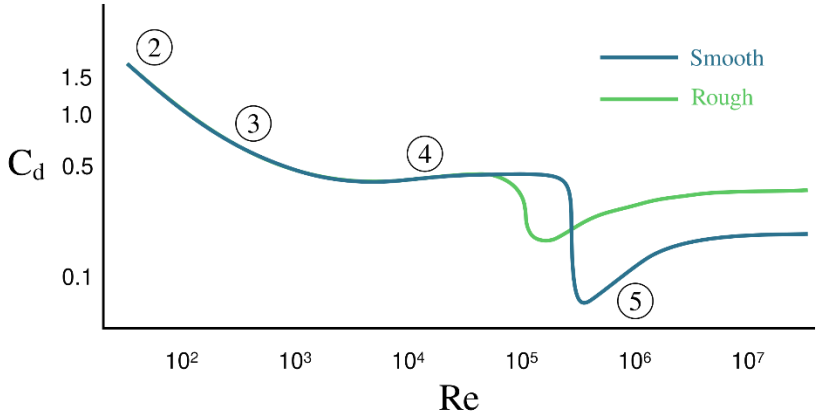

Figure 2-2 Drag coefficient as function of Reynolds number for smooth and rough single piles (source: Drag coefficient - Wikipedia). Offshore wind monopiles have a Re number of ~10^6-10^7.

2.3 CFD approach in software *TUDflow3D*

Open-source 3D CFD software TUDflow3D (De Wit,2015) is used in this study. It has been used successfully for density currents, rheological fluid mud flow, turbulent channel flow, flow past objects, monopile scour and many other flow cases (De Wit, 2015, Radermacher et al., 2016, De Wit et al., 2023). TUDflow3D solves the full, non-hydrostlatic 3D Navier Stokes equations including variable density via the mixture approach.

Large Eddy Simulation (LES) is used to capture turbulence. In LES, the larger turbulent eddies are solved on the grid and only the contribution of the non-resolved turbulent eddies, smaller than the grid size, is simulated by a sub-grid-scale model. We employ the often used WALE sub-grid-scale model (Nicoud et al., 1999) with $C_s = 0.325$. The turbulent eddy viscosity is added to the background molecular viscosity to form the total viscosity.

Validation of 3D CFD simulations with TUDFlow3D for flow past a monopile is provided in Appendix A.

3 Model approach

A numerical flume is set up to allow for a fair comparison between a high-resolution CFD model and the coarse-grid Wozep model. Its layout and implementation in the CFD and Delft3D-FM software, respectively, are described in Section 3.1. Section 3.2 gives an overview of the performed model scenarios, and finally Section 3.3 presents the analysis method with which we quantify mixing in both models.

3.1 Numerical flume layout

The numerical flume is three kilometres long and one kilometre wide, which corresponds to three adjacent computational cells in Wozep's DCSM-FM model (dark grey, Figure 3-1). The bed roughness is set at k_n = 0.07 m, which corresponds to Chezy = 65 $m^{0.5}$/s. The sides consist of free-slip closed boundaries and flow enters through the left-hand boundary at a depth-averaged velocity of 0.5 m/s. At both the inflow and outflow boundaries, the flow is given space to adjust and prevent interaction with the monopile structures (light grey, Figure 3-1). The monopiles have a diameter of 8 m, which is a typical value for new wind farms in the North Sea.

In this first exploration, we use a fixed ambient velocity, initial density profile and depth. Ideally, a wider parameter space would be examined, but given limited resources, we focus on one representative combination using ballpark values observed in several North Sea wind farms. The imposed upstream flow velocity of 0.5 m/s is within the typical range of 0.3-0.8 m/s observed in the Belgian OWF Norther (Hendriks, et al. 2025) and modelled at OWF Gemini (Zijl et al., 2023). We impose an upstream density profile that is representative for the stratification that is periodically observed at these locations for similar flow conditions. The salinity/density profile is based on a predecessor CFD simulation, in which a linear salinity/density profile of 32 PSU at the top and 33 PSU at the bottom is used as inflow condition and simulated for 2 km. The time-averaged vertical density profile after 2 km is used as input profile for both CFD and DFM production simulations used to assess the influence of monopiles. The water depth is 24 m throughout the domain, which is typical for the Dutch coastal North Sea area but relatively shallow for wind farms located further offshore. This choice is made to reduce computational cost, as CFD simulations become significantly heavier with increasing depth.

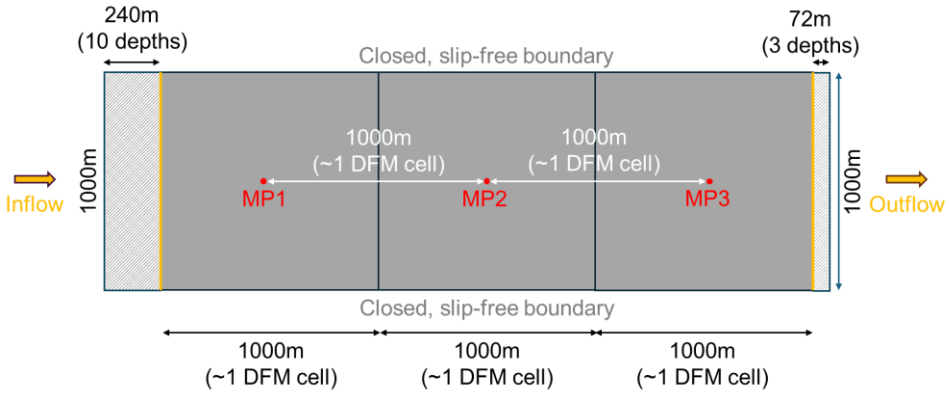

Figure 3-1 Model domain dimensions for CFD model. In Delft3D-FM an identical domain size is used, but the inflow and outflow areas (light grey) consist of an additional cell at both sides.

In CFD software TUDflow3D (version May 2025), the numerical flume is simulated using a high-resolution mesh. The grid size near the monopile is Δx = Δy = 0.32 m. This corresponds to 25 grid cells over the diameter of a monopile. Further away from the monopile, the horizontal grid size gradually increases to a maximum Δx = Δy = 1.92 m. The vertical grid size is Δz = 0.75 m, which corresponds to 32 layers in the vertical. The grid is designed such that the ratio of longest to smallest dimension of every grid cell remains below 3 which from our experience is important to capture turbulence adequately in the LES approach. The flow is given a distance of 10 respectively 3 water depths to adjust at the upstream and downstream boundaries (light grey, Figure 3-1).

The numerical flume in Delft3D-FM (version 2025.02), on the other hand, is presented as an extremely simplified grid. It has just five grid cells in the horizontal, each with Δx = Δy = 1 km, and 20 layers in the vertical. This resolution is nearly identical to that in the Wozep DCSM-FM model (Zijl et al., 2023). The 3 cells in the middle of this 2DV domain are the cells where the monopiles are placed for the scenarios, while the other 2 cells allow for 'free' flow before and after interaction with the monopiles.

3.2 Simulation overview

Five different monopile arrangements have been simulated, as summarized in Table 3-1.

In the three main simulations 1–3 (Table 3-1), the number of monopiles ranges from one to three. Simulation 1 places one monopile in the first square kilometer, simulation 2 adds one in the second, and simulation 3 assigns one to each square kilometer. The latter layout is depicted in Figure 3-1. In the Delft3D-FM implementation of these three cases, the drag coefficient C_D is fixed at the Wozep default value of 0.7.

As the monopile drag coefficient C_D is known to strongly affect mixing and stratification decay (Christiansen et al., 2023), the three main simulations were repeated with alternative drag coefficient values in Delft3D-FM. In this sensitivity analysis, we apply extreme values spanning the bandwidth reported in literature (see Section 2.2). Superscripts a and b in Table 3-1 denote lower and higher C_D values, 0.3 and 1.1, respectively.

Table 3-1 Overview simulated monopile arrangements. Superscripts a and b indicate that the Delft3D-FM simulation has been repeated with both a lower monopile drag coefficient Cd value of 0.3 and a higher Cd value of 1.1, respectively.

Simulation	#monpiles	Layout	Density (1/km^2)	Delft3D-FM monopile drag coefficient C_d	Delft3D-FM Domain width
1 [a, b]	1	In-line	1	0.7; [a]=0.3; [b]=1.1	1 cell
2 [a, b]	2	In-line	1	0.7; [a]=0.3; [b]=1.1	1 cell
3 [a, b]	3	In-line	1	0.7; [a]=0.3; [b]=1.1	1 cell
4	2	In-line	**2**	0.7	1 cell
5	2	*Side-by-side*	**2**	0.7	1 cell

Finally, two alternative monopile simulations were designed to test the influence of monopile layout on OWF mixing. This is done in the CFD model by placing two monopiles in one squared kilometer, either side-by side (simulation 5) or aligned in each other's wake 500 m apart (simulation 4). In Delft3D-FM, this distinction in monopile orientation cannot be made as the parameterization scales with the total monopile surface area – regardless of the layout within

one cell. Consequently, in Delft3D-FM simulations 4 and 5 are represented by one single simulation with a monopile density of 2 monopiles per km^2.

3.3 Quantifying mixing

In this study, stratification decay is used as a proxy for the OWF mixing energy. Stratification is quantified through the Potential Energy Anomaly (PEA) parameter (J/m^3) following the definition used in Simpson et al. (1978) and de Boer et al. (2008):

$$PEA = \frac{1}{H}\int_{-h}^{\eta} (\bar{\rho} - \rho) g z \, \mathrm{d}z$$

where g is the gravitational acceleration, $\bar{\rho}$ is the depth-averaged density, ρ is the fluid density that varies along coordinate z over the depth H, given by $H = \eta + h$, with η being the free surface and h the bed position.

PEA represents the energy required to mix a stratified water column to a uniform density $\bar{\rho}$. To account for the difference in grid resolution, we use the width-averaged potential energy anomaly over the numerical flume to compare Delft3D-FM and CFD results.

To distinguish OWF-induced mixing from natural mixing due to bed friction, we furthermore analyze stratification decline relative to a reference simulation without any monopile:

$$\Delta\, PEA = PEA_{\,with\ OWFs} - PEA_{\,reference}$$

Here ΔPEA is the decline in PEA caused by the presence of OWF's.

4 Results

Wozep's OWF mixing parametrization in DCSM-FM is evaluated by examining the detailed spatial development of stratification in the CFD simulations (Section 4.2), quantifying and comparing the parametrized decline in stratification (Section 4.3), assessing the sensitivity of the results to key model parameters (Section 4.4), and finally, by analyzing the relevance of different monopile layouts (Section 4.5). Before discussing the OWF-induced stratification decay, Section 4.1 first introduces what the flow field looks like in the wake of the monopiles.

4.1 Spatial development velocity and turbulence

The simulated spatial development of mean velocity and the total turbulent kinetic energy (TKE) around monopiles are shown in Figure 4-1 and Figure 4-2, respectively. Each monopile has a distinct downstream zone where the mean velocity is reduced (Figure 4-1) and converted into TKE (Figure 4-2). The velocity decay is strong in the first tens of meters, but quickly recovers leaving a moderate velocity decay in the order of 20% in a narrow zone downstream of the monopile (decrease of ~0.1 m/s, Figure 4-1). Furthermore, the CFD results show that turbulent kinetic energy dissipates after a few hundred meters, well before it reaches the downstream monopile (Figure 4-2). It is worth noting that advection of turbulent kinetic energy is explicitly resolved in CFD as turbulent addies are advected by the mean flow.

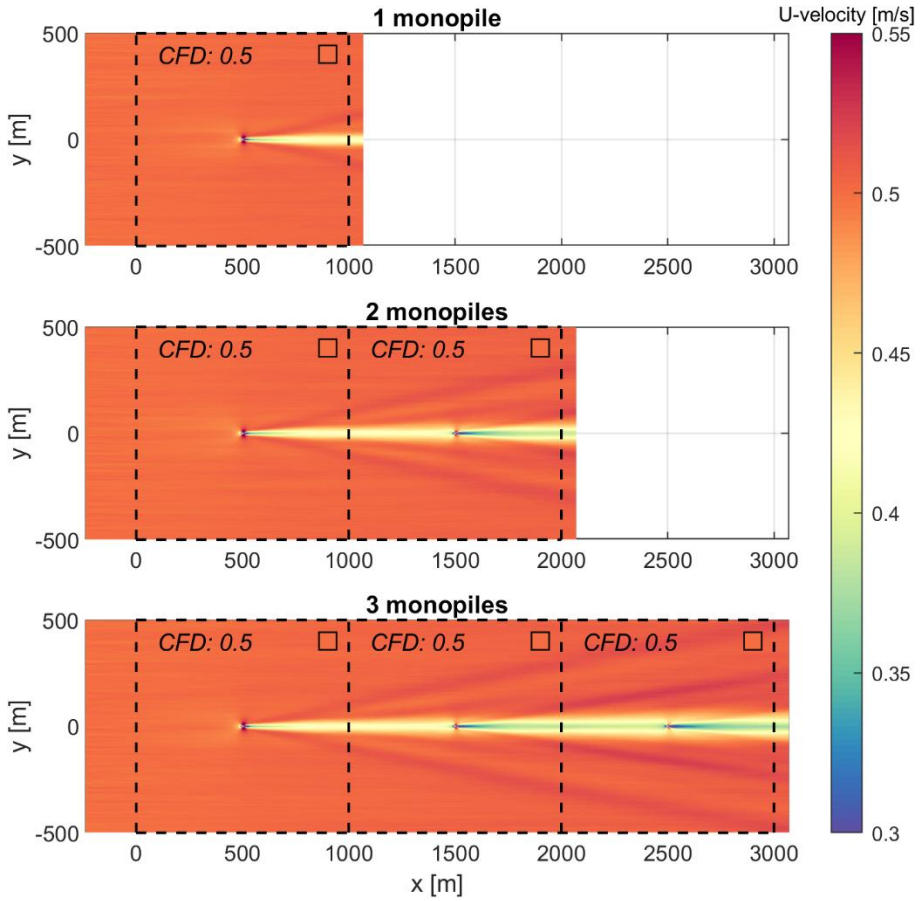

Figure 4-1 Spatial development of depth-averaged velocity in downstream direction for CFD simulations with respectively 1 monopile, 2 monopiles and 3 monopiles behind each other with a density of 1 monopile per km^2. Dotted contours indicate the size of computational cells in Delft3D-FM. The markers indicate the depth-averaged velocity based on CFD results (m/s) averaged over these areas of 1x1 km^2.

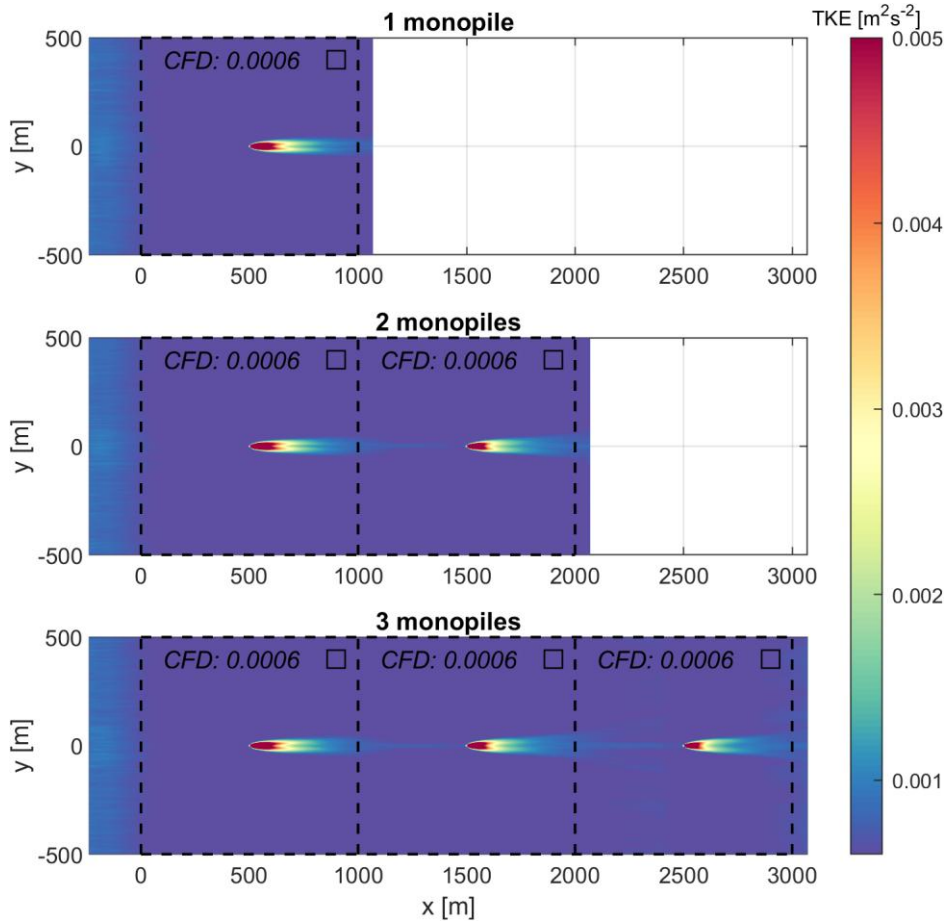

Figure 4-2 Spatial development of depth-averaged turbulent kinetic energy (TKE) for CFD simulations with respectively 1 monopile, 2 monopiles and 3 monopiles behind each other with a density of 1 monopole per km^2. Dotted contours indicate the size of computational cells in Delft3D-FM. The markers indicate the depth-averaged TKE based on CFD results (m^2/s^2) averaged over these areas of 1x1 km^2.

4.2 Spatial development stratification

The simulated spatial development of PEA around monopiles is shown in Figure 4-3 and Figure 4-4 for the five simulations in Table 3-1. Each monopile has a clear downstream zone in which the mixing induced by the monopile lowers the stratification and thus the PEA substantially. Close to the- monopile the PEA is lowered by the monopile induced turbulent mixing. Further downstream the zone of lower PEA expands in width induced by dispersion and lateral mixing. In this report we use the word ‘wake’ to describe this zone with reduced PEA downstream of a monopile, unless specified otherwise. Approximately 2.5 km downstream from a monopile the PEA wake reaches a width of 1 km. Hence, with a density of 1 monopile/km^2, the wakes from neighbouring monopiles will reach each other at this point. When monopiles are behind each other, the wake of the upstream monopile is not yet mixed over the lateral at the position of the next monopile at 1 km distance.

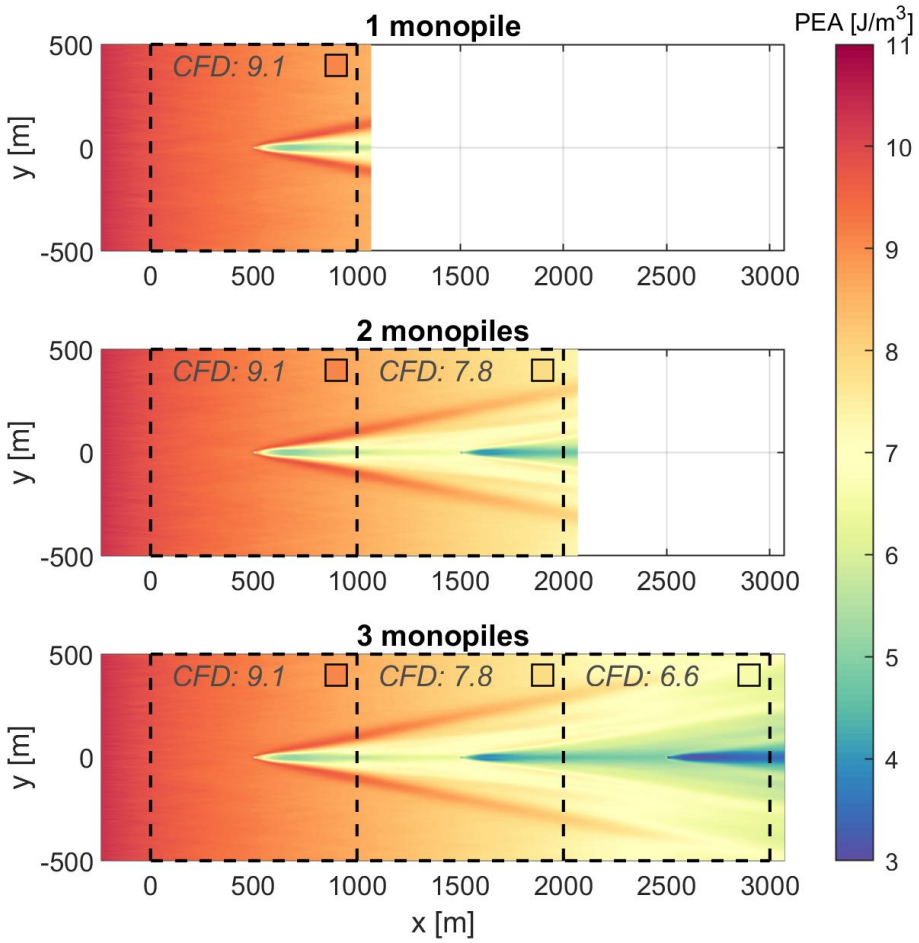

Figure 4-3 Spatial development PEA in CFD simulations with respectively 1 monopile, 2 monopiles and 3 monopiles behind each other with a density of 1 monopole per km^2 . Dotted contours indicate the size of computational cells in Delft3D-FM. The markers indicate the PEA based on CFD results (J/m^3) averaged over these areas of 1x1 km^2.

The biggest decline in PEA occurs directly downstream of the monopile. This is in line with field measurements at locations with similar water depths (20 to 30 m) and monopile widths (~8 m). Field measurements of PEA in the wake of a monopile in a Belgian windfarm (Hendriks et al. 2025), for instance, show a variation of 6.9 J/m^3 to 2.3 J/m^3. The higher values are found outside of the wake and the lower values are found within the wake. The measured drop of ~4.6 J/m^3 in PEA within the wake of an individual monopile is comparable to the simulated drop in the vicinity of the monopile (Figure 4-3). The simulated relative local decrease in PEA of ~40-50% is also in the same range as the measured decrease of 25-65% found in field measurements in the Danish North Sea (Dorrell, et al., 2022). Hence, these field measurements corroborate the CFD outcomes.

The position of monopiles relative to each other can affect how their wakes with reduced stratification overlap, and thus potentially interact, see Figure 4-4. When placed downstream of each other, the wakes overlap (bottom two panels), while for side-by-side placed monopiles wakes do not overlap when placed sufficiently far apart (top right panel).

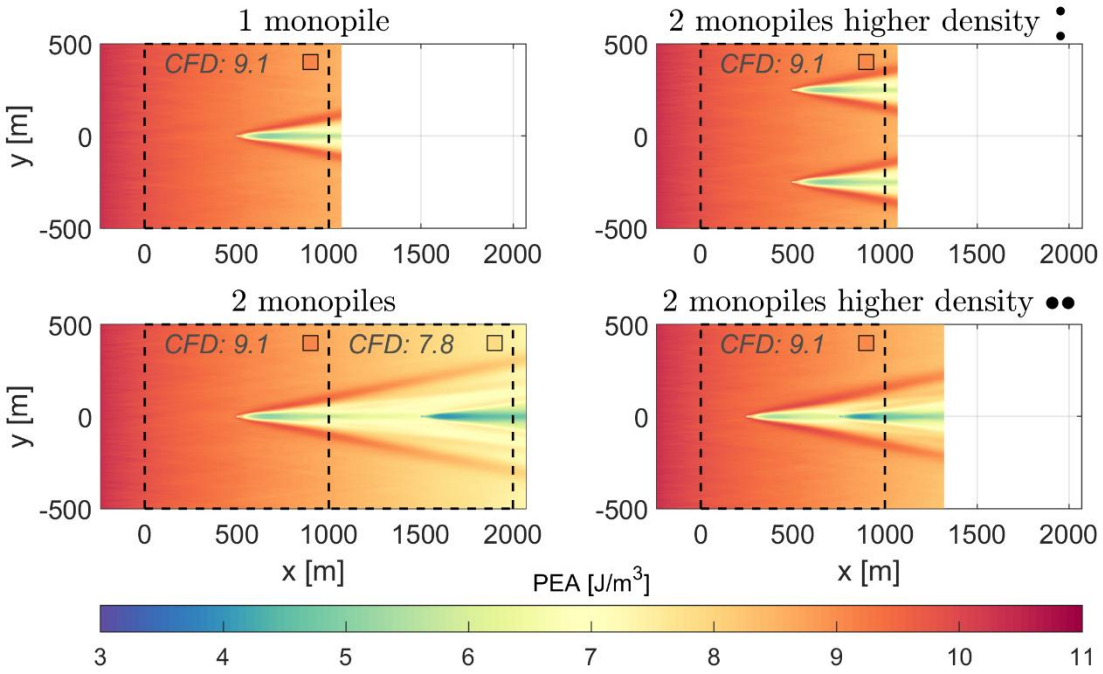

Figure 4-4 Spatial development PAE (J/m^3) in CFD simulations with 2 monopiles behind each other and side by side with a density of 2 monopole per km^2.

Also visible in Figure 4-3 and Figure 4-4 is that the ambient PEA in the simulations slowly decreases over distance, due to bed friction induced mixing. For that reason, the results in the remainder of this chapter are analysed by subtracting results with monopiles from reference simulation results without monopiles (ΔPEA).

4.3 Decay in stratification

The CFD results show that stratification decline varies strongly in space, with the spatial average about ten times smaller than the peak decline directly behind a monopile. Figure 4-5 shows this with both the spatially varying and averaged drop in PEA due to OWFs. The boxes in the upper right corner indicate the spatial-average decline for the corresponding Delft3D-FM cell ('DFM') and the area-average decline from the CFD model ('CFD'). The spatially-averaged decrease in PEA is in the order of 0.1 J/m^3 per monopile in the CFD results, whereas the maximum decrease can be as large as 5 J/m^3. Please keep in mind that the spatially-averaged decrease in PEA for the CFD model consists of the complete 1 km^2 around a monopile. This includes the upstream 500 m where no influence is present.

Delft3D-FM substantially overestimates the decay in stratification compared to the CFD model (Figure 4-5), as it predicts a decrease in stratification in the range of 0.5 - 1.5 J/m^3. These values are similar to the decrease in PEA within monopile wake (~100 m downstream), but are four to five times larger than the spatially-averaged PEA from the CFD model.

At the same time, the strong spatial variability in the CFD results suggests that also the spatially *averaged* CFD values may not be representative for local mixing processes. For example, localized mixing could already transport nutrients to the surface waters, where they may then be further dispersed, even if the area-averaged drop in stratification is small and would be insufficient to achieve this if applied uniformly.

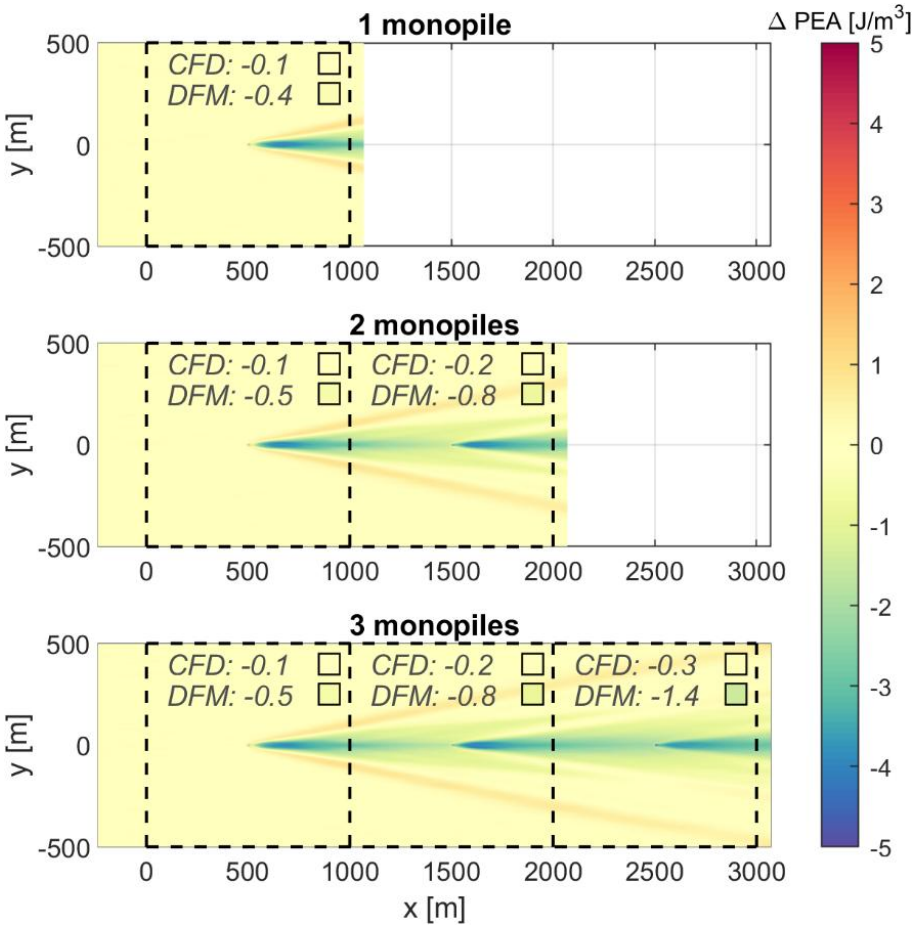

Figure 4-5 Spatial varying decrease in PEA for CFD simulations with respectively 1 monopile, 2 monopiles and 3 monopiles behind each other with a density of 1 monopole per km^2. Dotted contours indicate the size of computational cells in Delft3D-FM ('DFM'). The markers indicate the PEA decline (J/m^3) averaged over these areas of 1x1 km^2, based on CFD results and Delft3D-FM, respectively.

In the CFD model, each monopile reduces stratification, but the additional reduction contributed by each downstream monopile becomes smaller. Figure 4-6 shows that the width-averaged decrease in PEA of each monopile in the CFD model is approximately 0.17 J/m³ after the first kilometer, 0.1 J/m³ after the second, and only 0.06 J/m³ after the third. This is unlikely to be caused by a reduction in mixing for each extra monopile, since the increase in TKE caused by each monopile is similar see Figure 4-2. Instead, we hypothesize that the smaller reductions in PEA for subsequent monopiles occur because less stratification remains to be broken down, leading to an increasingly smaller decrease in PEA caused by subsequent monopiles.

In Delft3D-FM, the decline in stratification is stronger than in CFD, especially for multiple monopiles. Figure 4-6 shows that the PEA in Delft3D-FM further decreases (w.r.t. the reference simulation) in the cell downstream of the last monopile, but this cell does not contain a monopile (black line top panel, from -0.38 to -0.63 J/m^3). This additional decrease in PEA could potentially be caused by the advection of the additional turbulent kinetic energy from monopiles in the $k-\epsilon$ model. After all, in Delft3D-FM TKE is generated locally and subsequently advected in the $k-\epsilon$ transport equations. Only after two cells, at x=3000m, the stratification decline stabilizes in DFM. Some studies such as Rennau et al. (2012) disabled the advection of turbulent kinetic energy to study OWF mixing.

In the CFD model, the advection in turbulent kinetic energy is much less prominent (Figure 4-2) and consequently ΔPEA stabilizes within several hundreds of meters. This can be seen in Figure 4-6, as the blue lines quickly become horizontal.

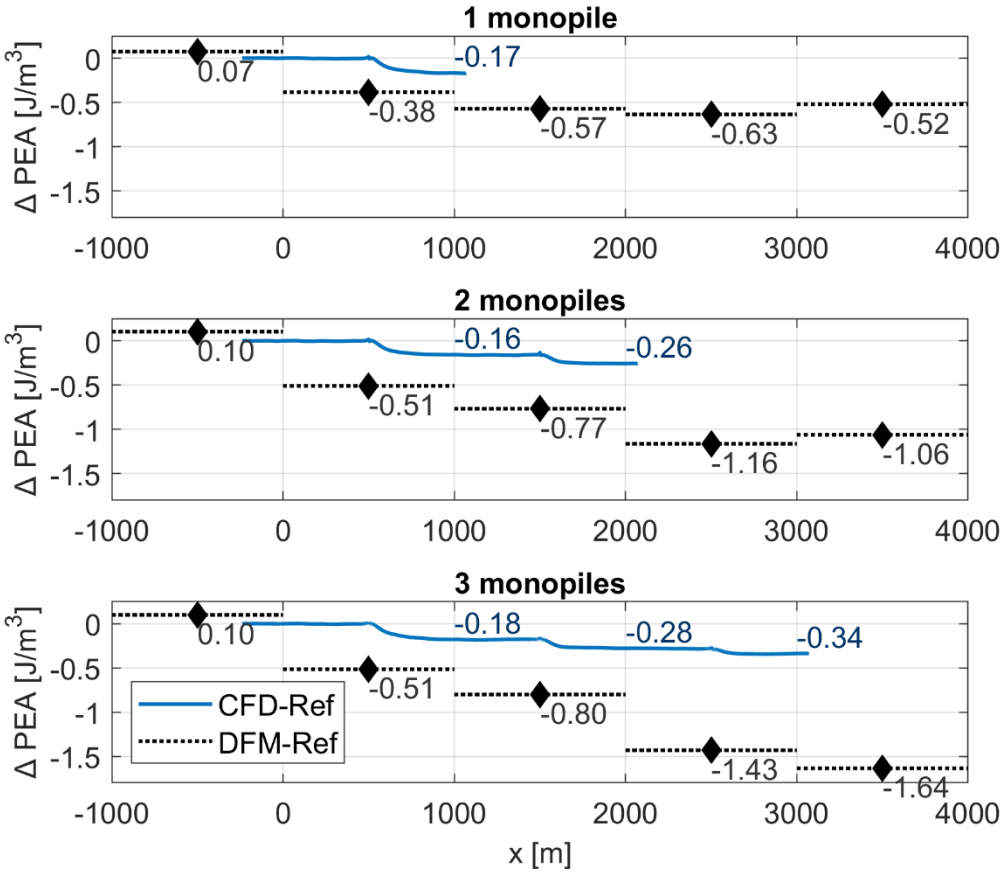

Figure 4-6 Width-averaged decrease in PEA for simulations with respectively 1 monopile, 2 monopiles and 3 monopiles behind each other with a density of 1 monopole per km^2. Black numbers indicate the discrete PEA drop based on Delft3D-FM, which are representative for a full cell area – indicated with horizontal black line. Blue lines denote the spatial variation in PEA decrease based on CFD results. The blue numbers indicate the PEA drop at precisely 1000, 2000 and 3000 m, which are different than the cell-area average values in Figure 4-5. Note that the OWF mixing parametrization in Delft3D-FM is only applied in cells where a monopile is present in CFD, visible as buckles in the blue line.

In the CFD results, the spatially-averaged decrease in stratification stabilizes after a few hundred meters downstream (Figure 4-6), but the wake with reduced stratification continues to widen over several kilometers (Figure 4-5). Turbulent mixing becomes weaker at distances of more than hundreds of meters from the monopile , see Figure 4-2, after which further widening of the wake is mainly due to dispersion of the stratification plume rather than active mixing. At a downstream distance of 2.5 km, the PEA wake reaches a width of approximately 1 km, meaning it would no longer be sub-grid in the Wozep model and would reach the PEA wake of neighboring monopiles at 1 km lateral distance.

4.4 Sensitivity to drag coefficient (C_d)

When the drag coefficient C_d is reduced from 0.7 to 0.3, the decay in stratification in Delft3D-FM is less overestimated and more in agreement with CFD results. This is shown in Figure 4-7, where it can be seen that the PEA drop for $C_d = 0.3$ (light grey line ▼) is reduced with 50%

compared to $C_d = 0.7$ (black line), suggesting an almost proportional response to changes in C_d. Similarly, increasing the drag coefficient to $C_d = 1.1$ leads to a stronger overestimation of the decay in stratification in Delft3D-FM (dark grey line ▲). The trends in PEA drop are similar for the different C_d, only with a different magnitude. The strong influence of C_D decay of stratification is in agreement with Christiansen et al. (2023) who showed that the PEA drop can increase as much as 100% when doubling C_D.

Interestingly, $C_d = 0.3$ is substantially lower than the drag coefficient applied in other large-scale studies investigating OWF mixing (Rennau et al., 2012; Carpenter, et al., 2016; Denis, et al., 2025), but it is in line with drag coefficients for a smooth pile at very high Reynolds number (Figure 2-2). Essentially, C_d depends on several numerical settings (e.g. cell size) and occurring physical conditions (e.g. flow velocities, marine growth). The specific range applicable to the Wozep DCSM-FM model warrants further examination as is proposed in the recommendations.

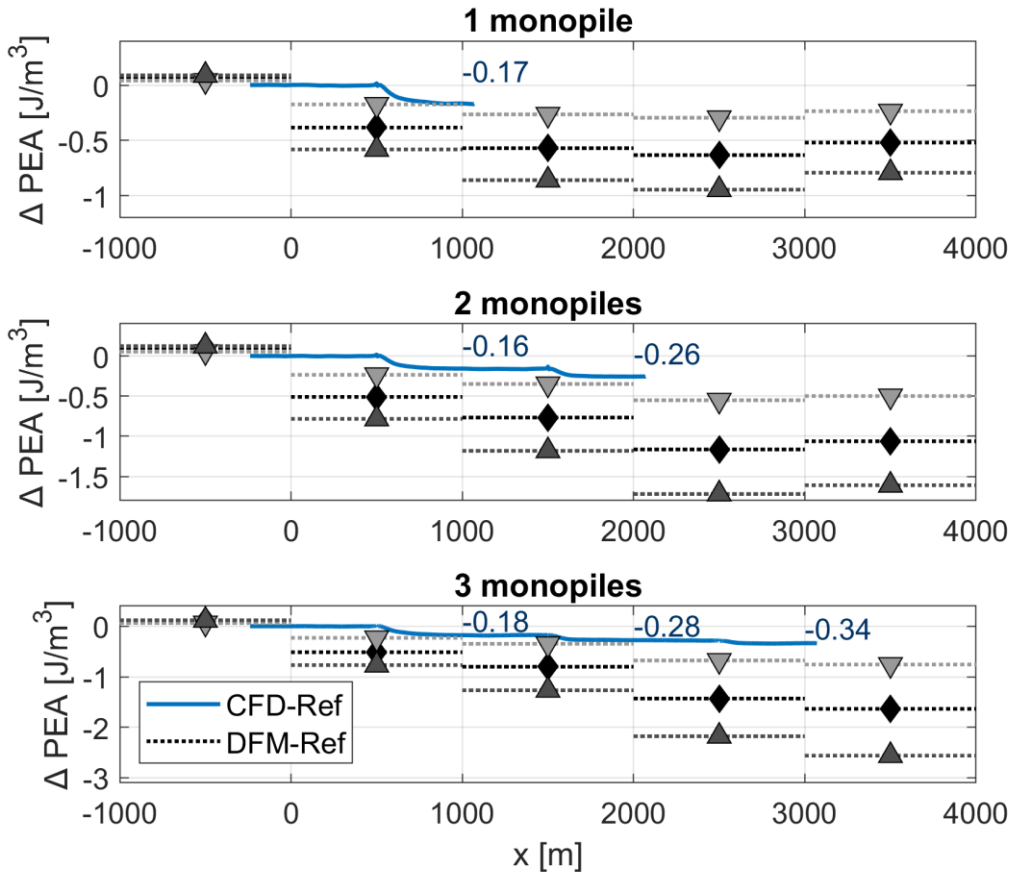

Figure 4-7 Width-averaged decrease in PEA for simulations for different monopile drag coefficients C_d applied in Delft3D-FM. Black line with a diamond icon shows the PEA drop for the Delft3D-FM run with a default value $C_d = 0.7$. The light grey (▼) and dark grey lines (▲) show the PEA drop for a lower and higher C_d of 0.3 and 1.1, respectively. Blue lines show the spatial variation in PEA decrease based on CFD results. Panels represent simulations with respectively 1 monopile, 2 monopiles and 3 monopiles behind each other with a density of 1 monopole per km2. Note that the OWF mixing parametrization in Delft3D-FM is only applied in cells where a monopile is present in CFD, visible as buckles in the blue line.

4.5 Influence monopile orientation and spacing

The influence of monopile orientation and spacing on stratification decline is illustrated in Figure 4-8. When the monopiles are 500 m side-by-side from each other the monopile PEA wakes do not interact in the first kilometer and the decline scales linearly with the number of monopiles (compare top panels). When two monopiles are behind each other the PEA wake of the second monopile starts within the PEA wake of the first monopile. This is more pronounced for a spacing of 500 m than at 1000 m.

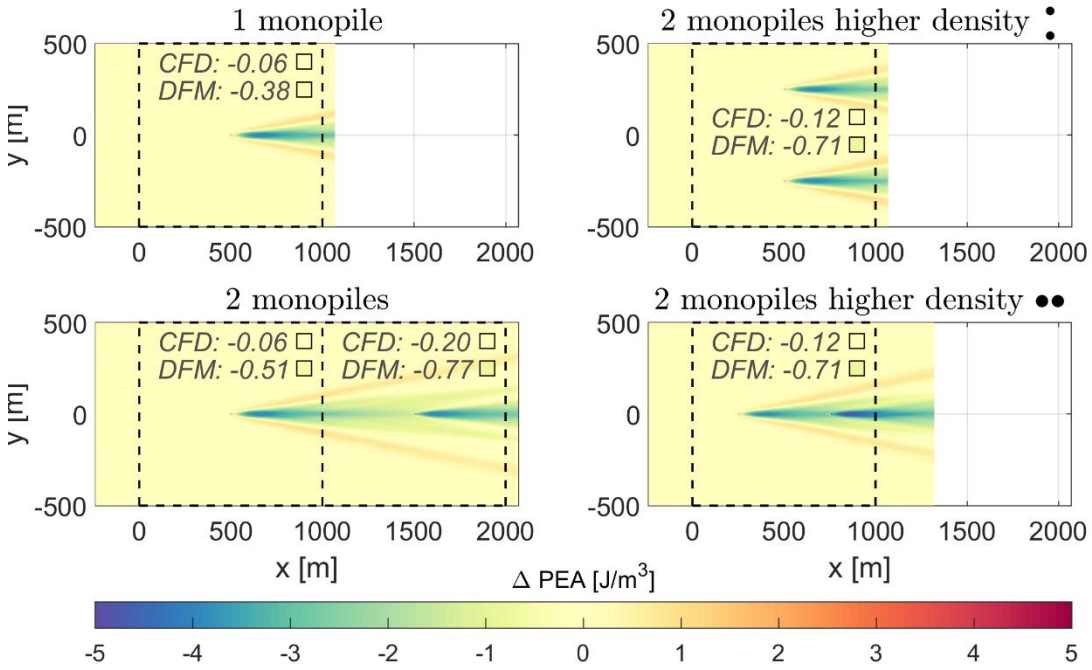

Figure 4-8 Spatial development PAE (J/m³) in CFD simulations with different layouts. Right: 2 monopiles behind each other (bottom) and side-by-side (top), both with a density of 2 monopile per km². Left: simulations with 1 and 2 monopiles behind each other at a density of 1 monopile per km².

The width-averaged PEA drops in Figure 4-9, show that monopile arrangement affects the efficiency of stratification mixing. The influence of two monopiles side-by-side, where the wakes do not interact, is almost double the influence of one monopile (drop of the yellow line is almost twice the drop of the blue line). This holds for both the absolute (Figure 4-9) and relative PEA drop (Figure 4-10). Hence, for monopile layouts where wakes do not interact, the stratification decline scales approximately linearly with monopile surface area. This is in agreement with the Wozep model parametrization, where turbulent mixing is proportional with the monopile surface area (Eq. 2-1). When two monopiles are placed side-by-side within 1 km², the resulting mixing is slightly greater than for monopiles aligned inline within 1 km², because less stratification remains available to be mixed for the 2nd monopile placed behind the 1st one (yellow line drops below orange line in top panel). This sensitivity for monopile orientation where wake interactions plays a role is not captured in the Wozep parametrization in Delft3D-FM.

The influence of distance between monopiles is subtle but present (bottom panel). Two monopiles at 1 km distance generate slightly less PEA drop than two monopiles at 0.5 km distance (0.26 vs 0.27 J/m³). Following the same rationale as above, this is explained by the background drop in PEA at larger downstream distances in the domain, which leaves less stratification to be mixed up by the second monopile. The relative drop in PEA, however, is slightly larger for two monopiles at 1 km distance compared to two monopiles at 0.5 km distance. This suggests that mixing efficiency is slightly reduced when monopiles are more

closely aligned. In the Wozep model, a higher monopile density results in a bigger initial PEA drop for the same number of monopiles. However, after 2 km the drop converges to identical values.

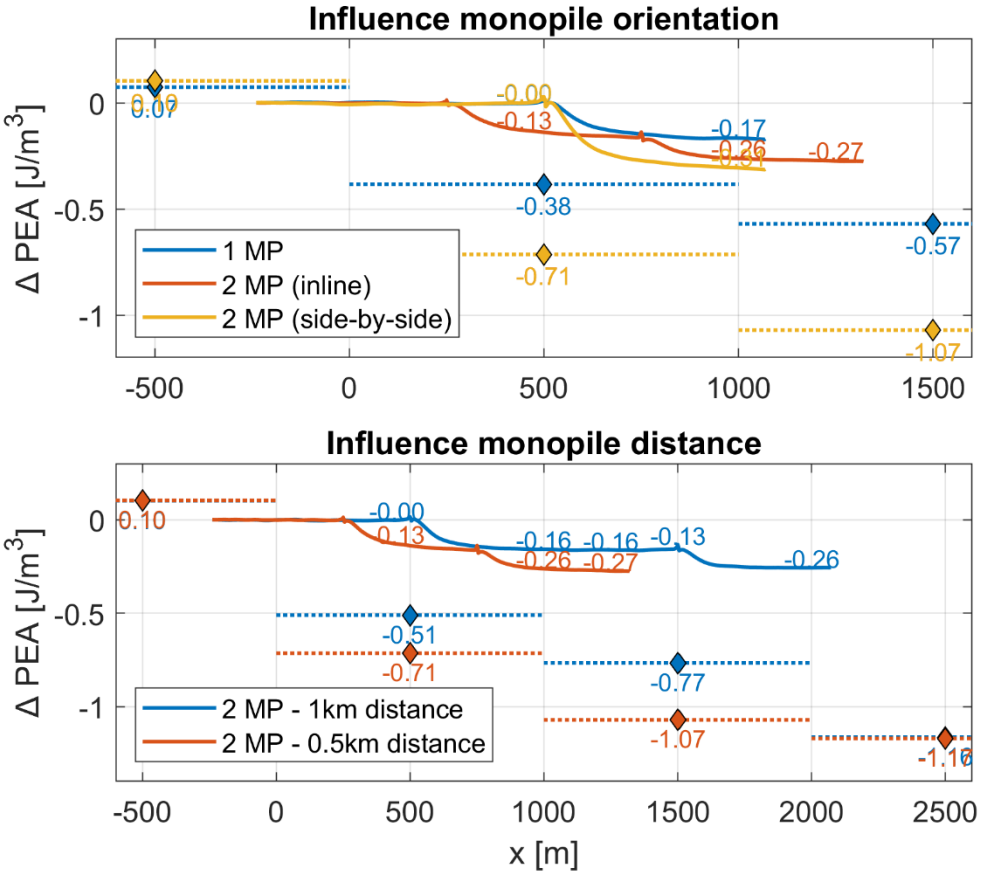

Figure 4-9 Influence of monopile layout on absolute, width-averaged PEA drop (J/m^3) for CFD (thick lines) and Delft3D-FM (dotted lines). Top panel: different orientations within 1 km^2. Bottom panel: influence spacing between two monopiles in line. Note that the OWF mixing parametrization in Delft3D-FM is only applied in cells where a monopile is present in CFD, visible as buckles in the solid lines.

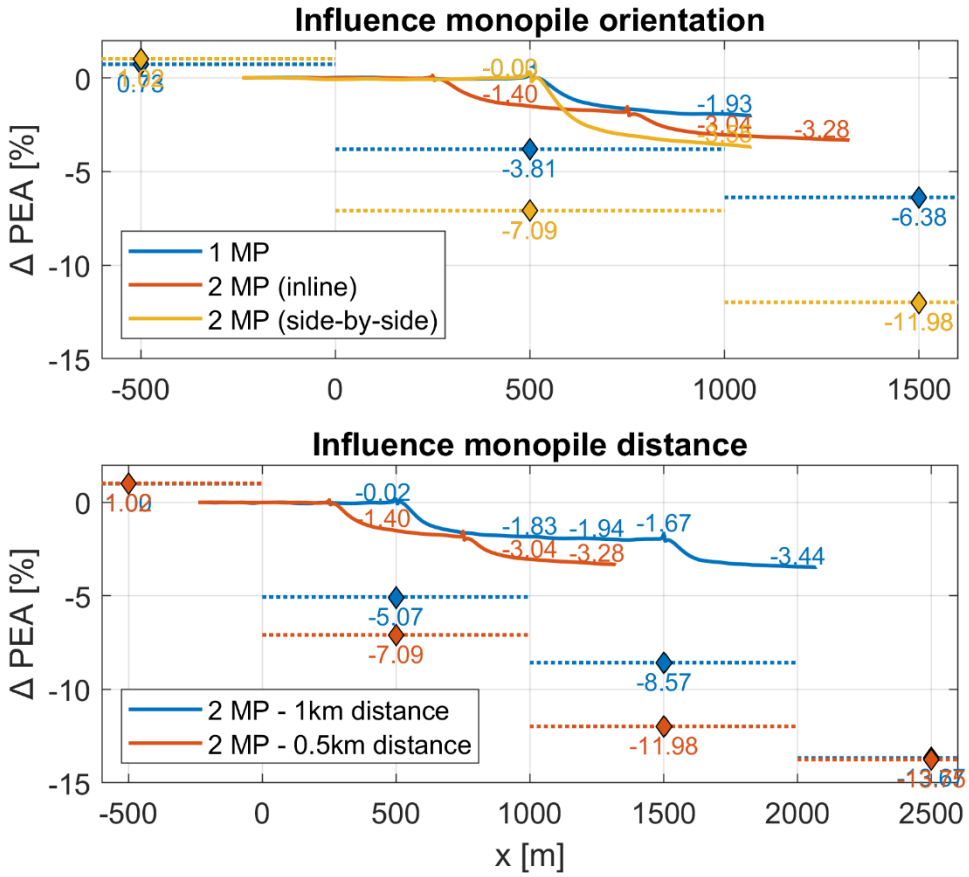

Figure 4-10 Influence of monopile layout on relative, width-averaged PEA drop (%) for CFD (thick lines) and Delft3D-FM (dotted lines). Top panel: different orientations within 1 km^2. Bottom panel: influence spacing between two monopiles in line. Note that the OWF mixing parametrization in Delft3D-FM is only applied in cells where a monopile is present in CFD, visible as buckles in the blue line.

5 Conclusion & recommendations

5.1 Conclusions

This study compared the Wozep offshore wind farm (OWF) mixing parametrization in Delft3D-FM with high-resolution CFD simulations under identical conditions. The CFD simulations provide realistic monopile-induced mixing, with stratification decay and wake expansion consistent with field observations.

For the idealized test conditions, the Wozep parametrization overestimates stratification decrease by roughly a factor of three to five compared to spatially-averaged CFD results. Sensitivity runs indicate a much better agreement with CFD when the drag coefficient is reduced from the default Wozep value of 0.7 to 0.3, although this value is substantially lower than those applied in other OWF mixing studies (Rennau, et al., 2012; Carpenter, et al., 2016; Denis, et al., 2025). The drag coefficient is a parameter with a clear but complex physical basis. It is influenced by the shape and the roughness of the object, and depends on the ambient hydrodynamic regime. Changing this parameter in models can be warranted, but needs to be based on physical arguments.

In Delft3D-FM, OWF presence further decreases stratification several kilometers downstream of monopiles, even in cells without monopiles. This appears to be related to the advection of turbulent kinetic energy and may contribute to the overestimation of mixing. In contrast, CFD results show that advection of turbulent kinetic energy vanishes after a few hundred meters, while the decline in stratification continues to spread mainly through advective and dispersive processes rather than active mixing.

Monopile orientation also has a subtle influence on mixing in CFD, with interacting wakes reducing efficiency per monopile. This effect is not fully captured in Wozep, where mixing scales only with total surface area, which is well representative for cases without substantial wake interaction. The relevance of stratification wake interaction can be further investigated in the Wozep DCSM-FM model for one complete windfarm with enhanced resolution and realistic flow conditions, as proposed in the recommendations.

Overall, this study has shown that, at monopile scale under idealized conditions, DCSM-FM yields a stronger stratification decrease than CFD and highlights several mechanisms that may contribute to the mismatch. The relevance and implications of these findings at full wind-farm scale and for water quality and ecology are expected to be location specific and warrant further investigation. Synergy can be sought with the NWA POWER programme, which aims to deepen understanding of key steering processes and to evaluate existing modelling approaches. Finally, our comparison between high-resolution CFD and coarse-grid model data has highlighted the importance of accounting for spatial variability, particularly when interpreting coarse EO datasets against model outputs, as localized influences of monopiles may remain undetectable at such scales.

5.2 Recommendations

Based on these findings, we recommend an end-to-end review of the Wozep OWF mixing parametrization to determine whether mechanistic refinements are needed, to assess potential implications for water quality results, and to validate CFD-based insights under a broader set of conditions.

- *Review Wozep DCSM-FM implementation of processes and sensitivity to key model parameters*.
  Evaluate the importance of different processes on the results. For example, assess whether it is feasible to switch off the advection of turbulent kinetic energy in Delft3D-FM, following the approach of Rennau et al. (2012) and Christiansen et al. (2023). Simultaneously, evaluate the influence of important model parameters on stratification decay and wake dynamics (e.g. $C_d, C_l, c_{\epsilon 2}$). Specifically, we advise to evaluate which value of C_d is appropriate for the Wozep DCSM-FM model considering the parameter's dependence on numerical settings (e.g. grid size) and physical conditions (e.g. flow velocities, depth, marine growth).

- *Extend the sensitivity analysis to water quality results to explore the bandwidth within which earlier Wozep conclusions may be influenced by the OWF parameterization*.
  As the drag coefficient C_d is known to have the strongest influence on stratification decay, we recommend rerunning the existing WOZEP North Sea model with an adjusted, lower drag coefficient to assess sensitivity of the previous water quality results to the OWF mixing parametrization.

- *Validate CFD-based insights with observational and model data under more realistic, spatially and temporally varying conditions.*
  Compare the Wozep North Sea model with a high resolution Delft3D-FM simulation of an individual wind farm to assess mixing in more realistic conditions with natural variability. This is similar to the approach in Denis et al. (2025), and allows us to assess monopile interaction and cumulative effects in more detail, whilst also informing the ongoing validation on how to deal with spatial variability in OWF effects. A useful intermediate step can be to apply the idealized Delft3D-FM configuration from this study at ~10 m resolution, resolving individual wakes and testing sensitivity to a broader set of ambient conditions (e.g. current speed and stratification).

6 References

Carmer, C. F. von, & Jirka, G. H. (2001). On turbulence and transport in shallow wake flows. *Proceedings of the 29th IAHR Congress*, Vol. B, pp. 80–86, Beijing, China.

Carpenter, J., Merckelbach, L., Callies, U., Clark, S., Gaslikova, L., & Baschek, B. (2016). Potential impacts of offshore wind farms on North Sea stratification. *PLoS ONE*.

de Boer, G., Pietrzak, J., & Winterwerp, J. (2008). Using the potential energy anomaly equation for tidal straining and advection of stratification in a ROFI. *Ocean Modelling*.

Deltares. (2025). *D-Flow Flexible Mesh: User Manual*. Delft.

Denis, P., Capet, A., Vanaverbeke, J., Kerkhove, T., Lacroix, G., & Legrand, S. (2025). Hydrodynamic alterations induced by floating solar structures co-located with an offshore wind farm. *Frontiers in Marine Science*.

Dorrell, R., Lloyd, C., Lincoln, B., Rippeth, T., Taylor, J., & Caulfield, C. (2022). Anthropogenic mixing in seasonally stratified shelf seas by offshore wind farm infrastructure. *Front. Mar. Sci.*

Füle, P., & Hernádi, Z. (2014). Investigation of turbulent channel flow using local mesh refinement. *Periodica Polytechnica Mechanical Engineering*.

Hendriks, E., Langedock, K., van Duren, L. A., Vanaverbeke, J., Boone, W., & Soetaert, K. (2025). The impact of offshore wind turbine foundations on local hydrodynamics and stratification in the Southern North Sea. *Frontiers in Marine Science*, 12:1619577. https://doi.org/10.3389/fmars.2025.1619577

Hinterberger, C. (2004). *Dreidimensionale und tiefengemittelte Large-Eddy-Simulation von Flachwasserströmungen* (Ph.D. thesis). Universität Karlsruhe.

Kernkamp, H. (2021). *Vegetation in DFM memo*. Delft: Deltares.

Meijer, D. (1998). *Modelproeven overstroomde vegetatie*. Lelystad: HKV Lijn in Water.

Nicoud, F., & Ducros, F. (1999). Subgrid-scale stress modelling based on the square of the velocity gradient tensor. *Flow, Turbulence and Combustion*, 62(3), 183–200.

Radermacher, M., De Wit, L., Winterwerp, J. C., & Uijttewaal, W. S. J. (2016). Efficiency of hanging silt screens in crossflow. *Journal of Waterway, Port, Coastal and Ocean Engineering*, 142(1).

Simpson, J., Allen, C., & Morris, N. (1978). Fronts on the continental shelf. *Journal of Geophysical Research*, 83(C9), 4607–4614.

van Duren, L., Zijl, F., Leummens, L., van Kessel, T., Jaksic, L., Vilmin, L., & Heye, S. (2025). *Impacts of offshore wind development on the North Sea ecosystem*. Deltares.

van Duren, L., Zijl, F., van Kessel, T., van Zelst, V., Vilmin, L., van der Meer, J., et al. (2021). *Ecosystem effects of large upscaling of offshore wind on the North Sea – Synthesis report*. Deltares.

Wit, L. de, Broekema, Y., & Plenker, D. (2023). 3D CFD LES process-based scour simulations with morphological acceleration. *11th International Conference on Scour and Erosion*, Copenhagen.

Wit, L. de. (2015). *3D CFD modelling of overflow dredging plumes* (Ph.D. thesis). Delft University of Technology, Delft.

Zijl, F., Laan, S., Leummens, L., Zijlker, T., van Kessel, T., van Zelst, V., et al. (2023). *Scenario studies on potential ecosystem effects in future offshore wind farms in the North Sea*. Deltares.

A Validation CFD model for flow past circular pile

Experimental data which measured flow and turbulent quantities at distances up to 15 water depths, corresponding to 25 pile diameters in the experiment, are used to validate the used CFD model TUDflow3D. Also the sensitivity to grid size is investigated by using different grid sizes in the simulations. The experiment is documented in Hinterberger (2004) and Carmer und Jirka (2001) and has the following characteristics:

- Re_D=9030
- Re_H=5440
- D/h=1.66
- Hydraulic smooth wall

The CFD TUDflow3d results are obtained with LES and the monopile captured with a first order immersed boundary method and a gridsize $\Delta x = \Delta y = D/70$ in the vicinity of the monopile and uniform $\Delta z = D/53$, with D being the monopile diameter. The instantaneous flow field and vortex street are clearly visible in the instantaneous simulation results shown in Figure 6-1 and Figure 6-2. These figures nicely illustrate how unlike the Reynolds Averaged Navier Stokes (RANS) approach, the Large Eddie Simulation (LES) approach resolves the larger turbulent eddies and as such simulates the intermittent turbulent flow in the wake.

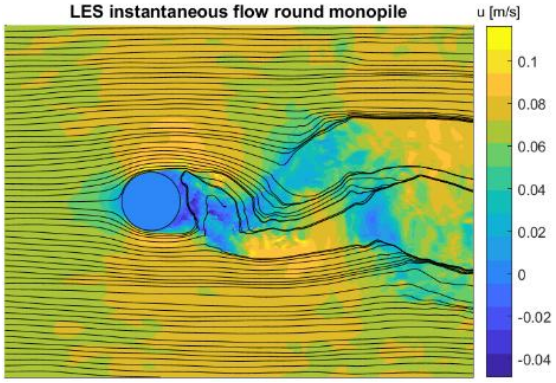

Figure 6-1 Simulated instantaneous streamlines and streamwise velocity with LES model

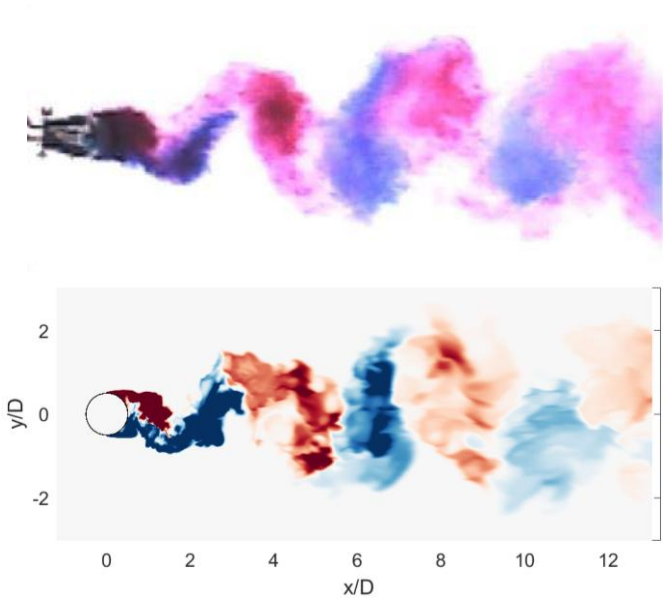

Figure 6-2 Coloured dye indicating the vortex street behind the circular cylinder experiment (top) and LES simulation (below). Please note that the moment of this snapshot of the experiment and of the LES simulation are not exactly the same

A quantitative comparison with the measured flow and turbulent quantities is provided in Figure 6-3. The model underpredicts the flow velocities in the wake 5 water depths downstream of the pile and accurately captures the flow velocities in the wake at larger distances of 10 and 15 water depths (corresponding to 16 and 25 pile diameters in the experiment). The turbulent fluctuations (u') in the wake are overpredicted by the model. Turbulent fluctuations (v') are overpredicted 5 water depths downstream, but correctly simulated at 10 and 15 water depths downstream. The results are very similar in quality to LES simulations with a boundary following grid of Hinterberger (2004) with similar resolution.

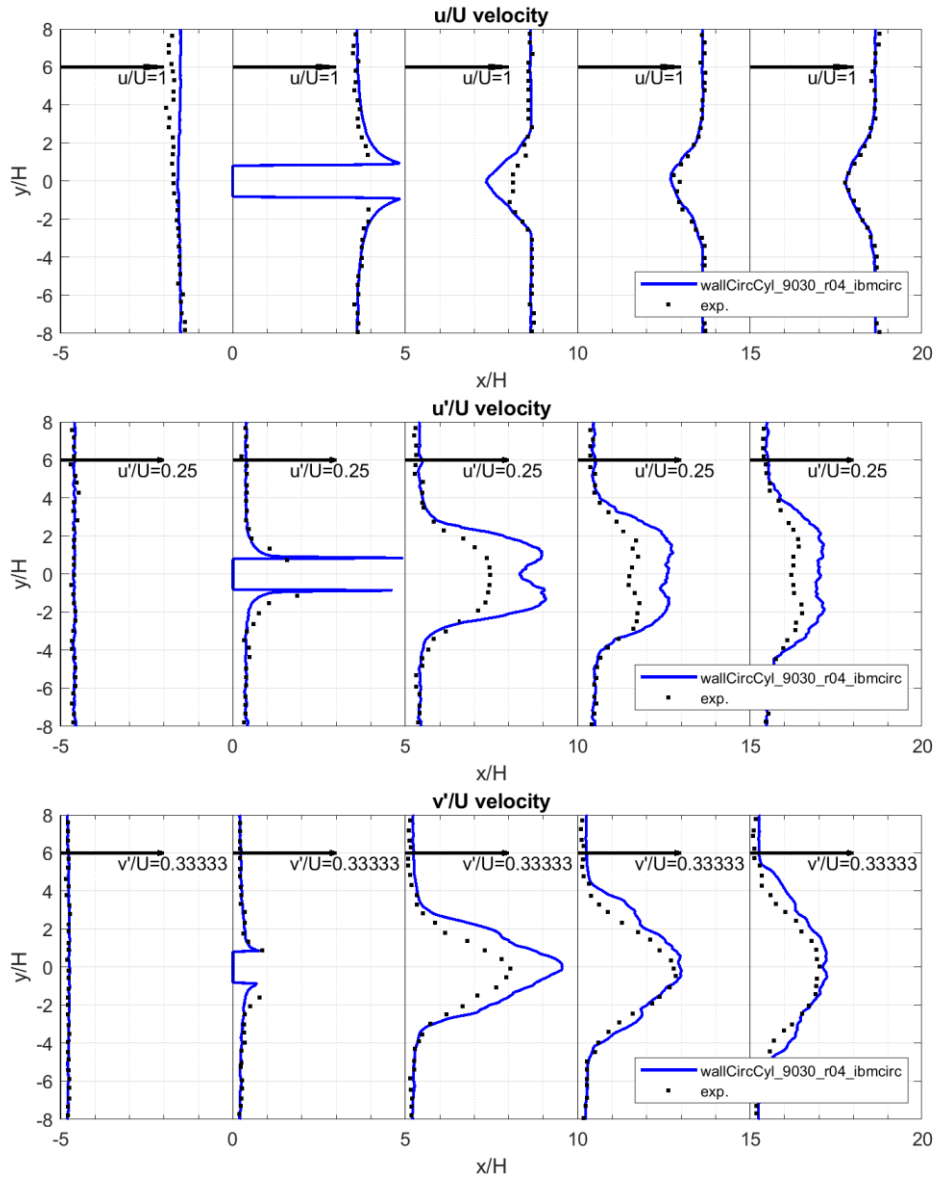

Figure 6-3 Comparison LES CFD (default resolution) flow past a round pile results to experiment

Grid size dependency has been verified by running this case with three different resolutions:

- Fine grid [r04 in legend] : Δx,Δy=D/70 (near monopile) and Δz=D/53 (uniform)
- Medium grid [r04m in legend] : Δx,Δy=D/40 (near monopile) and Δz=D/53 (uniform)
- Coarse grid [r04c in legend] : Δx,Δy=D/25 (near monopile) and Δz=D/30 (uniform)

Figure 6-4 illustrates that the results are hardly dependent on the tested grid sizes. Hence, the grid resolution of $\Delta x, \Delta y = D/25$ as used in the Wozep CFD simulations is adequate to assess the mixing induced by a monopile.

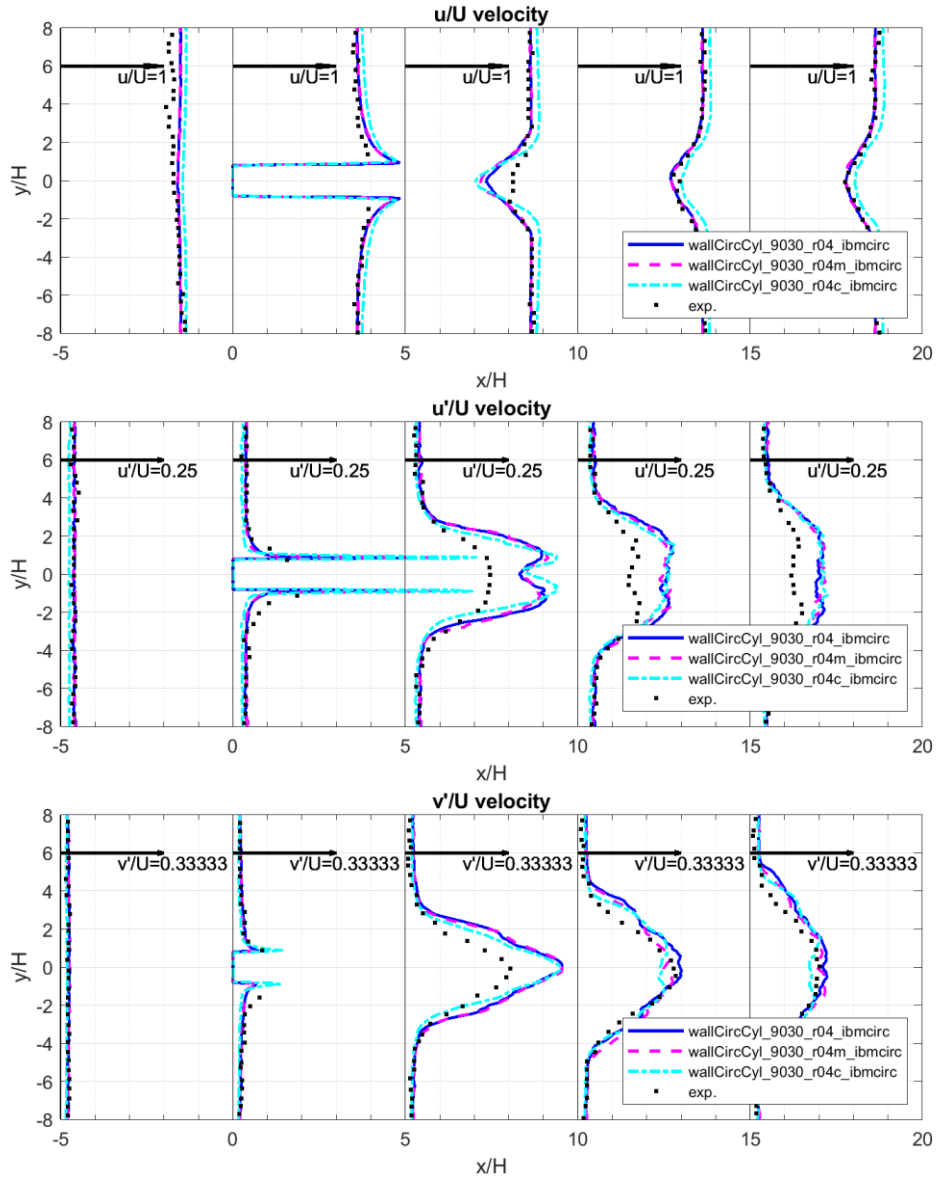

Figure 6-4 Grid size sensitivity LES CFD for flow past a round pile

Deltares is een onafhankelijk kennisinstituut voor toegepast onderzoek op het gebied van water en ondergrond. Wereldwijd werken we aan slimme oplossingen voor mens, milieu en maatschappij.

Deltares

www.deltares.nl